BIOCHEMISTRY
including biophysical chemistry & molecular biology

Article

pubs.acs.org/biochemistry

Molecular Features of Product Release for the PKA Catalytic Cycle

Adam C. Bastidas,[†] Jian Wu,[†,‡] and Susan S. Taylor*[,†,‡,§]

[†]Department of Pharmacology, University of California, San Diego, San Diego, California 92093, United States
[‡]Department of Chemistry and Biochemistry, University of California, San Diego, San Diego, California 92093, United States
[§]Howard Hughes Medical Institute, University of California, San Diego, San Diego, California 92093, United States

Supporting Information

ABSTRACT: Although ADP release is the rate limiting step in product turnover by protein kinase A, the steps and motions involved in this process are not well resolved. Here we report the apo and ADP bound structures of the myristylated catalytic subunit of PKA at 2.9 and 3.5 Å resolution, respectively. The ADP bound structure adopts a conformation that does not conform to the previously characterized open, closed, or intermediate states. In the ADP bound structure, the C-terminal tail and Gly-rich loop are more closed than in the open state adopted in the apo structure but are also much more open than the intermediate or closed conformations. Furthermore, ADP binds at the active site with only one magnesium ion, termed Mg2 from previous structures. These structures thus support a model where ADP release proceeds through release of the substrate and Mg1 followed by lifting of the Gly-rich loop and disengagement of the C-terminal tail. Coupling of these two structural elements with the release of the first metal ion fills in a key step in the catalytic cycle that has been missing and supports an ensemble of correlated conformational states that mediate the full catalytic cycle for a protein kinase.

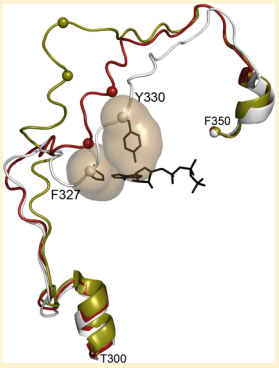

Protein kinases are an important family of enzymes that govern many signaling processes within cells by transferring the γ-phosphate of ATP onto a substrate protein. The addition of a phosphate group produces large and diverse effects on the modified proteins but is often associated with activating or inhibiting a cellular process. Because of the vast importance of protein kinases in cellular processes, dysfunctional kinase signaling can lead to several diseases including cancer.[1] Protein kinases are thus important drug targets, and better understanding of kinase structure, function, and catalysis will advance our strategies for drug targeting.

cAMP-dependent protein kinase, also called protein kinase A (PKA), is one of the most well-studied protein kinases, and because of the high conservation of the protein kinase family, it serves as a model for all protein kinases.[2] Under nonactivating conditions, PKA exists as a heterotetrameric holoenzyme complex composed of a regulatory (R) subunit dimer that binds and inhibits two catalytic (C) subunit monomers. PKA is activated by cAMP, which binds to the R-subunits and releases the inhibition of the C-subunits.[3] Once released from R-subunit inhibition, the active C-subunits can phosphorylate target proteins at membranes, in the cytoplasm, and in the nucleus. In many cases, PKA is targeted to a specific site where it is dedicated to the regulation of a colocalized protein. The C-subunit of PKA was the first kinase structure solved,[4] and this structure defined the bilobal architecture that is shared by all protein kinases. These lobes were termed the N-lobe (or small lobe) and C-lobe (or large lobe). Many subsequent crystal structures defined the wide range of conformations adopted by the dynamic protein kinases. The C-subunit has been crystallized in several states termed "open," "closed," and "intermediate" based on the relative orientation of the N- and C-lobes. The open conformation adopts the largest distance between the N- and C-lobe and was observed with the apo C-subunit and with the C-subunit bound to an inhibitor peptide IP20.[5,6] The closed conformation displays tight packing between the N-lobe and the C-lobe, which causes a closing of the active site cleft and the exclusion of water, and this conformation is typically seen when the protein is crystallized with IP20 and ATP or ATP analogues.[7] A representative intermediate conformation was observed when the C-subunit was crystallized with adenosine;[8] however, there is clearly an ensemble of intermediate conformations. These crystal structures, as well as NMR data,[9] demonstrate that the C-subunit adopts a wide ensemble of conformations, and these dynamics and conformations contribute to the regulation of enzyme activity.

The kinetics and phosphoryl transfer reaction by PKA are also well-characterized, and these studies have improved our understanding of kinase reaction progression.[10] Pre-steady-state and steady-state kinetics of PKA showed that phosphoryl transfer of the γ-phosphate of ATP onto the substrate is a very rapid event; it is other processes that govern the rate of the reaction. These rate-limiting steps are also regulated by magnesium ion.[11] Most protein kinases, including PKA, require magnesium to bind ATP and catalyze phosphoryl transfer under physiological conditions. At low magnesium concentration (0.5 mM), PKA has a higher turnover rate than at high

Special Issue: New Frontiers in Kinases

Received: June 3, 2014
Revised: July 31, 2014
Published: July 31, 2014

   dx.doi.org/10.1021/bi500684c | *Biochemistry* 2015, 54, 2−10

magnesium concentration (10 mM), and at the low magnesium concentration, the turnover rate is governed partially by ADP release and partially by conformational changes that occur before and after phosphoryl transfer.[12−14] At high magnesium ion concentrations, the PKA reaction rate is governed by ADP release[11,15,16] and the conformational changes that are associated with ADP release. Therefore, ADP release is one of the most important steps in PKA reaction turnover and is highly influenced by the magnesium ions.

PKA binds two magnesium ions, which were termed Mg1 and Mg2. Mg1 binds in a bidentate manner with Asp184 of the "DFG" motif as well as the β- and γ-phosphates of ATP. Mg2 coordinates with one oxygen atom of Asp184, with Asn171, and with the α- and γ-phosphates of ATP.[17,18] Each magnesium ion also binds water molecules to fulfill an octahedral coordination state.[19] The nomenclature of these magnesium ions as Mg1 and Mg2 was made based on an older crystal structure that reported electron density for mostly one magnesium ion when the C-subunit was crystallized with a low concentration of magnesium.[18] The ion that showed more electron density was thus termed Mg1 because it was thought to bind first or more strongly with ATP, and the other ion was termed Mg2. Despite this nomenclature, recent studies suggest that the designation of the two Mg ions most likely does not correlate with the order in which they bind. Another crystal structure of the C-subunit obtained under low magnesium concentration shows electron density for only one magnesium ion, but the ion observed in the crystal structure corresponds to the Mg2 ion.[20] Furthermore, other protein kinases such as CDK2 often crystallize with one magnesium ion, and the ion observed is analogous to Mg2.[21] Finally, separate crystal structure studies of reaction progression by PKA and CDK2 both identify Mg2 as the ion that likely remains in the active site following phosphoryl transfer while Mg1 is lost, suggesting that Mg2 may be the more stably bound ion.[22,23] In contrast, loss of Mg1 may be an important part of the rate-limiting step of ADP release and may explain the slower turnover rate at high magnesium concentration due to continued occupancy of both metal binding sites.

To further elucidate reaction progression by PKA and the conformations involved in the reaction trajectory, we obtained the first crystal structure of the C-subunit bound only to ADP by soaking apo crystals with ADP and magnesium. No crystal structures of the C-subunit bound only to ATP or ADP were previously solved because the inhibitor peptide, IP20, is generally necessary to crystallize PKA with nucleotide. There is a structure of the C-subunit bound only to adenosine.[8] However, adenosine lacks the phosphate groups, and therefore, it lacks information about the magnesium ions and lacks information on reaction turnover since adenosine is not a naturally bound product. Here we report the apo structure of the C-subunit refined to 2.9 Å resolution and the ADP bound structure refined to 3.5 Å resolution. The ADP bound structure supports previous findings that ADP binds with Mg2. Also, the ADP bound structure adopts a conformation that does not conform to the "open", "closed", or previously solved "intermediate" states, and therefore, the structure further defines the conformational flexibility of the protein and provides insights into the motions and mechanisms that may govern ADP release. These structures highlight in particular the dynamic nature of the C-tail and show how its motions and functions are correlated with the Gly-rich loop. Both motifs are highly ordered and linked in the closed conformation. In the ADP bound structure, the C-tail is disordered, the Gly-rich loop is open, and the two motifs are not coupled. The order−disorder transition of the C-tail and its role in the recruitment and release of nucleotides from the active site is clearly highlighted in the ensemble of structures described here.

MATERIALS AND METHODS

Purification of the Myristylated C-Subunit Protein. The myristylated K7C C-subunit was prepared by coexpression with yeast NMT as described previously[24] and purified following a method described previously.[25] The K7C mutant was used for crystallization because it increases the yield of the myristylated protein. The myristylated protein was used for crystallization because the apo structure was initially obtained to characterize the role of N-myristylation in PKA structure.

Crystallization and ADP Soaking. The apo myristylated K7C C-subunit crystallized under similar conditions utilized for the previous apo WT nonmyristylated C-subunit structure.[5] The protein was dialyzed overnight into 50 mM bicine, 150 mM ammonium acetate, 10 mM DTT, pH 8.0. Then the protein was concentrated to approximately 8−10 mg/mL. The protein was setup for crystallization using the hanging drop vapor diffusion method at 4 °C. The protein was screened against different well solutions with 2-methyl-2,4-pentanediol (MPD) concentrations ranging from 2% to 18% and with 9−13% methanol added to the well solution immediately before sealing the well. The crystals were obtained using 8 μL drops of 1:1 volume of protein solution to well solution. Crystals typically appeared in 1−2 months, unlike the previous apo C-subunit structure, which reported crystal appearance in 6−12 months.[5] The apo myristylated K7C C-subunit structure was obtained from a crystal grown with a well solution containing 8% MPD and 9% MeOH added to the well. The protein crystallized contained two sites of phosphorylation on Thr197 and Ser338.

Attempts to cocrystallize the C-subunit with ADP were unsuccessful. Therefore, in order to obtain an ADP bound structure, the apo crystals were soaked with ADP and $MgCl_2$. A solution of ADP and $MgCl_2$ was prepared in 0.1 M Tris buffer at pH 7.0 and added to the crystal drop to yield a final drop concentration of approximately 5 mM ADP and 5 mM $MgCl_2$. The crystals were allowed to soak for 24−48 h before being harvested and flash frozen. The structure reported here was obtained from a crystal soaked with ADP/$MgCl_2$ for 48 h.

Data Collection and Refinement. The crystals were flash cooled in liquid nitrogen with cryoprotectant solution (16% MPD and 15% glycerol). Data was collected on the synchrotron beamline 8.2.1 of the Advanced Light Source, Lawrence Berkeley National Laboratories (Berkeley, California). The crystal structures were integrated using iMOSFLM.[26] The protein crystallized in the $P2_1$ space group as with the previous apo structure. Molecular replacement was carried out using Phaser[27] with the previously solved apo C-subunit structure, PDB ID 1J3H,[5] as a search model for the apo structure and with the apo structure solved here as the search model for the ADP bound structure. The refinement was performed using refmac5,[28] and model building was done in Coot.[29] Refinement was performed using a TLS and restrained refinement along with noncrystallographic symmetry (NCS) restraints. The TLS groups and NCS restraints used corresponded to the small lobe (residues 10−126 and 327−350) and large lobe (residues 127−326). The apo and ADP bound structures were refined to R_{work}/R_{free} of 24.4%/29.2%

dx.doi.org/10.1021/bi500684c | Biochemistry 2015, 54, 2−10

Table 1. Crystallography Data Collection and Refinement Statistics[a]

	apo	ADP bound
PDB ID	4NTS	4NTT
space group	$P2_1$	$P2_1$
cell dimensions		
a (Å)	50.96	50.48
b (Å)	142.61	143.15
c (Å)	63.16	62.57
α, β, γ (deg)	90, 103.61, 90	90, 103.61, 90
unique reflections	19,014 (2,818)	10,660 (1,572)
multiplicity	3.1 (3.1)	2.7 (2.7)
resolution range (Å)	61.38−2.90 (3.06−2.90)[b]	32.15−3.50 (3.69−3.50)[b]
R_{merge} (%)	5.1 (44.1)	10.5 (48.6)
I (σI)	9.7 (2.1)	5.7 (2.4)
completeness (%)	97.7 (99.0)	97.5 (98.4)
R_{work}/R_{free} (%)[c]	24.4/29.2	22.7/28.4
avg temp factors (B factors) for all atoms (Å^2), chain A/chain B		
all residues	72.2/69.0	103.2/99.7
N-lobe (residues 1−126)	72.1/77.8	104.3/104.4
C-lobe (residues 127−300)	65.2/55.1	97.3/91.2
C-tail (residues 301−350)	96.2/96.6	121.4/118.5
near FDDY (residues 320−335)	117.2/134.4	133.9/130.5
ADP	NA	161.8/124.2
magnesium	NA	62.2/78.8
Ramachandran angles (%)[d]		
favored regions	93.66	91.54
allowed regions	100	100
rms deviations		
bond lengths (Å)	0.006	0.007
bond angles (deg)	1.013	1.114

[a]Data collection was performed at ALS laboratory in Berkeley, CA on beamline 8.2.1. [b]Values in parentheses correspond to the highest resolution shell. [c]To calculate the R_{free}, 5% of the data was excluded from the refinement . [d]Ramachandran plot quality as defined in MolProbity.[30]

and 22.7%/28.4%, respectively. The data collection and refinement statistics are shown in Table 1 with Ramachandran values as defined in MolProbity.[30]

PDB Deposition. The coordinates and structure factors for the apo and ADP bound structures were deposited into the RCSB PDB with accession codes of 4NTS and 4NTT, respectively.

RESULTS

Apo C-Subunit Structure. The myristylated C-subunit of PKA was crystallized in an apo state to determine any effects of myristylation in the absence of ligands. A K7C mutant was crystallized because it increases the yield of the myristylated protein.[25] The apo crystal structure was refined at 2.9 Å resolution (Table 1, Figure 1A). There is electron density for myristic acid in one of the two molecules in the asymmetric unit (ASU); however, there is density for only 4 of the 14 carbon atoms of myristic acid (Figure 1B). The lack of electron density for myristic acid implies that the myristic acid group binding within the hydrophobic pocket could be involved in forming a closed state since there is more electron density for the myristic acid group in structures that adopt a closed conformation, particularly in the binary complex that contains only peptide, compared with the open conformation adopted here in an apo state.[25] The lack of density likely reflects high flexibility or disorder of the myristyl group, and this flexibility may correlate with different steps of the catalytic cycle.

The overall structure of the myristylated apo C-subunit reported here is in an open conformation similar to the previous WT nonmyristylated apo structure (1J3H).[5] There are two molecules in the ASU that are similar to each other with an RMSD of 0.66 Å between chain A and chain B when aligned by the whole protein (Figure 1A). The structure is very similar to the previous apo structure with a few differences. For example, the Cys199 residue was modified with β-mercaptoethanol in the previous apo structure and is unmodified in this structure. This caused some small shifts in the residues at the activation loop in the structure reported here compared with the previous structure, and the position of the residues in this structure are more likely to represent the native apo conformation since modification of Cys199 renders the C-subunit inactive.[31] Furthermore, the previous structure showed electron density for 2-methyl-2,4-pentanediol (MPD) in the myristic acid pocket, but since our structures used the myristylated protein, instead there is electron density that corresponds to the myristic acid group in chain A and no electron density in the myristic acid pocket in chain B. Finally, the C-tail was not modeled in the previous apo structure due to lack of electron density. Although the electron density of the C-tail in this structure is also very poor with little density for residues 318−330 in both molecules, we did model the C-tail into the structure. However, the C-tail is still not well resolved, the temperature factors are very high, and there is also no clear density for the side chains (Table 1, Figure 1C). The modeled C-tail should be interpreted as showing the tentative location of

dx.doi.org/10.1021/bi500684c | Biochemistry 2015, 54, 2−10

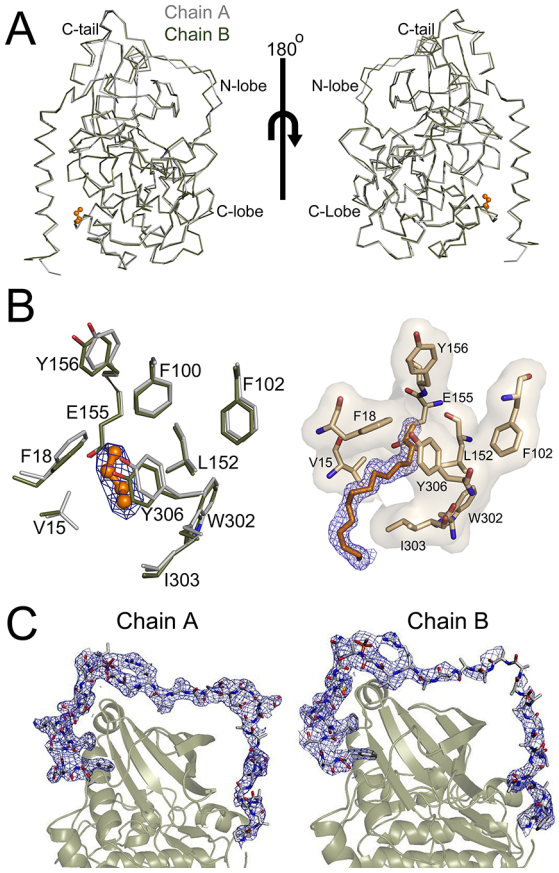

Figure 1. Apo structure of the catalytic subunit of PKA. (A) The overall apo structure is displayed in ribbon representation with chain A colored gray and chain B colored olive and with chains A and B aligned by the entire protein. (B) (left) The myristic acid binding pocket for chains A and B, which are colored as in panel A, is displayed along with the $2F_o - F_c$ electron density at 1σ shown in blue for the myristic acid group from chain A. There is no electron density for myristic acid in chain B. (right) In contrast, the $2F_o - F_c$ electron density at 1σ is visible for the entire myristic acid group in the closed state (4DFX).[25] (C) The $2F_o - F_c$ electron density at 1σ is shown in blue for the C-terminal tail of chains A and B.

the backbone of this region of the protein. The fact that the C-tail is disordered may cause disordering of other regions in the apo protein. The side chain of Arg56 is disordered here, whereas in the closed conformation this arginine interacts with Glu333 in the C-tail. This arginine is one link between the C-tail and the Gly-rich loop, and this communication is lost in the apo conformation when the C-tail becomes disordered. Although the apo structure did not show enhanced stability of the myristylated N-terminus nor show large differences compared with the previous apo structure, it did allow us to ask about ADP binding and release since this has been a key missing step in the reaction pathway.

Overall ADP Bound C-Subunit Structure. The ADP bound structure of the C-subunit was obtained by soaking apo crystals with Mg/ADP and was refined to 3.5 Å resolution (Table 1). The overall ADP bound structure is most similar to the apo structure with an RMSD of 0.74 Å between the apo and ADP bound structures aligned by the entire protein using both molecules in the ASU. The two molecules in the ASU of the ADP bound structure are similar to each other with RMSD values between chain A and chain B for the overall protein of 0.61 Å. ADP and one magnesium ion are present in both molecules in the asymmetric unit (Figure 2). The main differences between chain A and chain B occur at the Gly-rich loop and C-terminal tail.

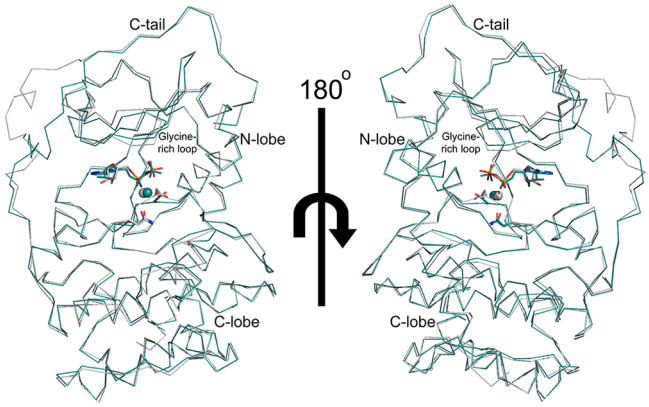

Figure 2. ADP bound structure of the C-subunit of PKA. The overall ADP bound structure of the C-subunit is displayed in ribbon representation with chain A colored gray and chain B colored cyan, and the two molecules from the asymmetric unit are aligned by the entire protein. ADP from each molecule is displayed in stick representation and colored by element, Asn171 and Asp184 that bind to the magnesium are displayed in stick representation and colored by element, and the magnesium ion is colored by chain and displayed in sphere representation.

As with the apo structure, the electron density of the C-terminal tail is not strong, but there was enough electron density to model the approximate location of the peptide backbone. Also, the C-terminal tail typically forms part of the adenine binding pocket when the C-subunit is bound to nucleotide. In chain B, there was some positive electron density in the region that Phe327 and Tyr330 typically occupy when bound to nucleotide without the C-tail modeled, and there is some electron density with the C-tail modeled with the residue side-chains at this location using omit maps. Therefore, the side chains of these amino acid residues are modeled in the structure for chain B and show how these two aromatic side chains bind ADP (Figure 3A). Mutagenesis of either of these residues leads to severe defects in activity.[32−34] In chain A, the C-tail does not form part of the binding site, and this is due most likely to close crystal packing at the C-tail with a symmetry related molecule (Figure 3A,B). Another difference between chain A and chain B is the conformation of the Gly-rich loop. Residues 50−53 are much lower in chain A than chain B, especially Ser53. It is possible that Ser53 helps to bind to ADP more in chain A than chain B because of the lack of the C-tail forming part of the binding site (Figure 3C).

ADP and one magnesium ion are present at the active site in both molecules in the ASU, and there is strong electron density to validate their presence (Figure 4). Before ADP and magnesium were included in the structure, there was strong positive electron density for ADP/Mg in both molecules in the ASU, and the final electron density for ADP/Mg, as modeled, is convincing (Figure 4). However, the electron density is better in chain B than in chain A, and correspondingly, the B-factor values are higher for the ADP/Mg in chain A than chain B (Table 1). It is possible that the better electron density in chain B is because the C-tail can form part of the ADP binding pocket in chain B but not chain A. Therefore, this adds credence to the

dx.doi.org/10.1021/bi500684c | *Biochemistry* 2015, 54, 2−10

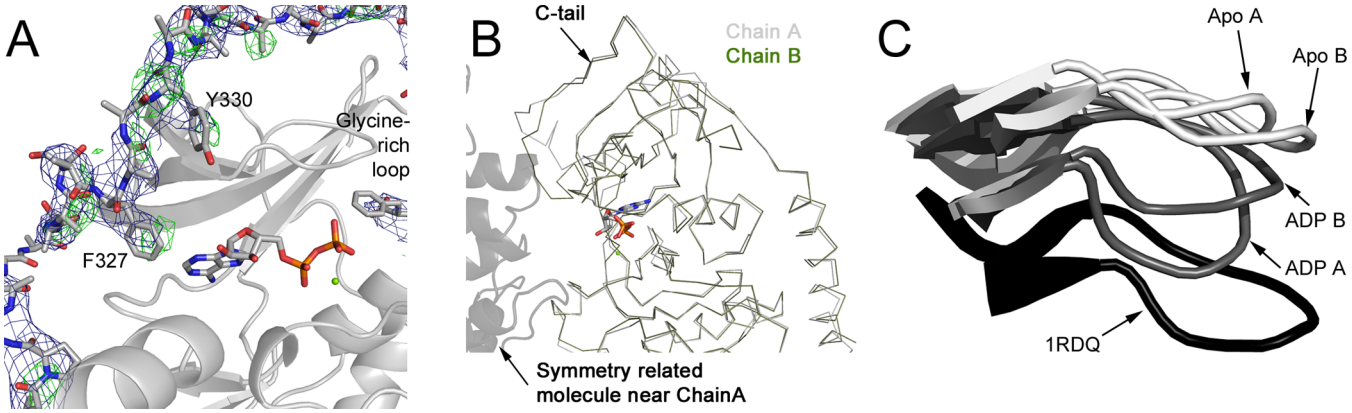

Figure 3. Changes at the C-terminal tail and Gly-rich loop in the ADP bound structure. (A) The $2F_o - F_c$ electron density at 1σ is displayed in blue for the C-terminal tail of chain B from the ADP bound structure, and the resulting $F_o - F_c$ electron density map contoured to 2.5σ is displayed in green for the C-tail from chain B when the C-terminal tail is excluded from the final model of the structure. (B) Chain A, gray, and chain B, olive, are displayed is ribbon representation and aligned by the entire protein. A symmetry related molecule near the C-terminal tail of chain A is displayed in black transparent cartoon representation showing that crystal packing prevents chain A from adopting the C-tail conformation adopted by chain B. (C) The apo structure, the ADP bound structure, and a ternary structure, 1RDQ,[7] were aligned by the entire protein, and the location of the Gly-rich loop from each structure following this alignment is displayed.

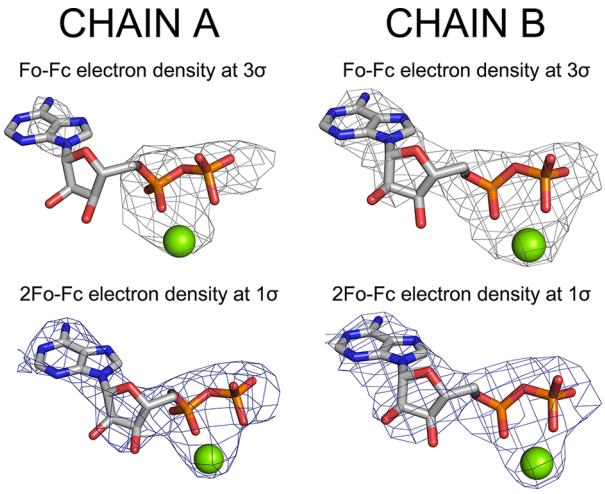

Figure 4. Electron density for ADP from each molecule in the asymmetric unit. The $F_o - F_c$ electron density at 3σ from the first refinement of the ADP bound structure without ADP or magnesium modeled into the structure is displayed for chains A and B (top), and the $2F_o - F_c$ electron density of the final model contoured to 1σ is displayed for each chain (bottom).

importance of these residues for binding to nucleotide, which was also verified with mutagenesis previously[32−34] and with hydrogen−deuterium exchange coupled to mass spectrometry measured with the C-subunit bound to ADP.[35]

Despite binding to ADP, the C-subunit still adopts a largely open conformation. The Gly-rich loop is still raised much more than the closed state, although it is lowered compared with the apo state (Figure 5A,B). Similarly, the C-terminal tail forms part of the binding site for ADP in chain B, but the C-tail does not close down onto the active site to the same extent in the ADP bound structure as it does in the closed state (Figure 5A−C). Therefore, the ADP bound structure adopts a conformation that does not conform to any of the previously identified states, open, closed, or intermediate. This fact is further illustrated by examining different distances between residues or regions of the protein that characterize the different states (Table 2). These distances are different in the ADP bound structure than in the open, closed, or intermediate states. Therefore, the ADP bound structure displays a new conformation of the C-subunit that could represent a conformation involved in ADP release. Additionally, there are differences in each molecule in the ASU suggesting that these could represent an ensemble of intermediate states during ADP release.

Mg Binding Site and Implications on Reaction Progression. There is only one magnesium ion present in the ADP bound structure unlike typical PKA ternary structures, which display two magnesium ions at the active site.[7] The magnesium ion at the active site in the ADP bound structure corresponds to Mg2. Although the location of the magnesium ion does not exactly match the typical position of Mg2, the magnesium ion is clearly situated between Asp184 and Asn171, which would correspond to the Mg2 ion (Figure 6A). To further verify that the magnesium ion is modeled correctly and corresponds to Mg2, the magnesium ion was removed from the final model of the structure, which was then refined. The corresponding $F_o - F_c$ map shows strong positive electron density at the site where the magnesium ion was modeled, and again, the site corresponds to Mg2 based on its location between Asp184 and Asn171 (Figure 6B). Therefore, Mg2 is the ion that binds more strongly with ADP and verifies previous studies suggesting that Mg1 is lost following phosphoryl transfer.[22,23]

DISCUSSION

The apo and ADP bound structures provide several insights into PKA structure, conformational dynamics, and reaction progression. Although the myristylated apo structure presented here is similar to the previous apo structure,[5] it provides important new information. For instance, the myristic acid group is more disengaged from the enzyme in an apo state than in the ligand bound states based on very little or no electron density for the myristic acid group for chain A and chain B, respectively. This lack of density suggests that the myristyl moiety is disordered in an apo state and may become more ordered or more tightly anchored to the protein in the presence of ligands. Comparing the apo state to the ADP bound structure also highlights the disorder to order transition of the C-tail, which coordinates with many other regions of the

dx.doi.org/10.1021/bi500684c | Biochemistry 2015, 54, 2−10

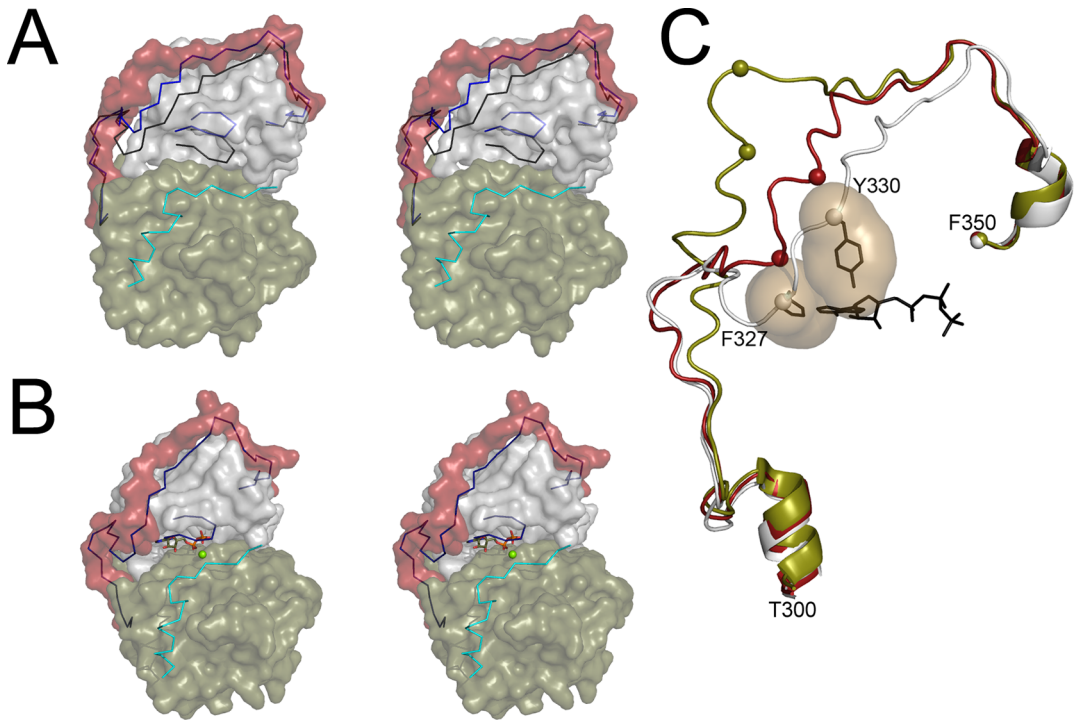

Figure 5. ADP bound structure adopts a unique conformation. (A) A stereoview of the apo structure reported here is displayed in surface representation with the N-lobe (residues 1−126) colored gray, large lobe (residues 127−300) colored olive, and C-tail (residues 301−350) colored red. Chain B from the ADP bound structure and a ternary structure, 1RDQ,[7] are aligned with the apo structure by the entire protein. The C-tail and Gly-rich loop from the ADP bound structure are colored blue and shown in ribbon representation, and the C-tail and Gly-rich loop from the ternary structure are colored black and displayed in ribbon representation. The inhibitor peptide, IP20, from the ternary structure is colored cyan and shown in ribbon representation. (B) A stereoview of chain B from the ADP bound structure is displayed in surface representation with the regions of the protein colored as in panel A. The C-tail and Gly-rich loop from the ternary structure, 1RDQ, aligned with the ADP bound structure by the entire protein are shown in ribbon representation and colored blue. IP20 is depicted as in panel A. (C) The dynamic nature of the C-tail. The ADP bound structure, colored red, adopts a conformation that does not conform to the open state colored olive, or the closed state colored gray. The residues Phe327 and Tyr330 are displayed in surface representation which are important for ATP binding, colored black.

Table 2. Distances within the C-Subunit That Define Different Conformations[a]

conformation:	ADP bound (chain A/B)	open	intermediate	closed	closed	closed
peptide	none	IP20	none	IP20	IP20	IP20
nucleotide	ADP	none	adenosine	ATP	none	AMP-PNP
PDB ID	4NTT	1CTP	1BKX	1ATP	1APM	1CDK
His87−Thr197 (N-PO_4)	6.7/6.3	7.1	3.2	2.7	2.8	2.8
Glu170−Tyr330 (backbone C═O−OH)	NA/12.3	14.6	8.6	8.2	8.2	7.9

[a]Adapted from Johnson et al.[2]

protein. The C-tail and Gly-rich loop are tightly coupled to ligand binding and are better resolved and more tightly coupled together in the presence of ligands. Finally, the ADP bound structure provides a glimpse into the motions and steps that may govern reaction progression by PKA and likely many, if not all, protein kinases.

The ADP bound structure displays one magnesium ion bound at the active site that corresponds to Mg2, which is situated between Asp184 of the DFG motif and Asn171 (Figure 6A,B). This structure suggests that PKA binds ADP with Mg2, and therefore, Mg1 must be released following phosphoryl transfer. This mode of reaction progression was seen previously in both CDK2 and PKA.[22,23] Crystal structures showed that ADP can bind with one or two magnesium ions at the active site of PKA or CDK2, and if only one magnesium ion is bound, the ion corresponds to Mg2. Release of Mg1 is therefore hypothesized to be an important part of the rate-limiting step of ADP release. Furthermore, computational studies that investigated the mode of ADP release from PKA with two magnesium ions bound suggested that ADP release was so energetically unfavorable that it was nearly impossible without release of one or both magnesium ions.[16] This structure supports the previous findings and hypothesis because PKA binds to ADP with one magnesium ion corresponding to Mg2.

An examination of several kinase structures bound to ADP suggests that many kinases may release Mg1 following phosphoryl transfer or bind Mg2 more strongly than Mg1. Several kinase structures crystallized with ADP show two magnesium ions at the active site that correspond to Mg1 and Mg2.[23,36,37] In other cases, when a kinase binds one magnesium ion at the active site, the ion bound corresponds to Mg2.[23,38−41] Therefore, it is likely that many protein kinases bind two magnesium ions to facilitate phosphoryl transfer. Kinases can then retain both ions following phosphoryl transfer or can release one ion, the Mg1 ion, to facilitate ADP release. There are, however, some kinase structures bound to ADP that

dx.doi.org/10.1021/bi500684c | *Biochemistry* 2015, 54, 2−10

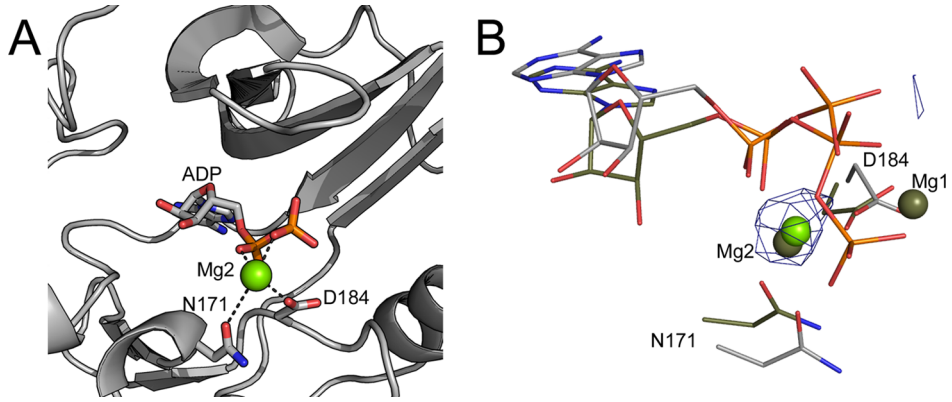

Figure 6. ADP binds at the active site with Mg2. (A) The active site of chain B from the ADP bound structure is displayed in cartoon representation with ADP displayed in stick representation and magnesium displayed in sphere representation. The side chain of Asn171 and Asp184, which chelate the magnesium ions, are displayed in stick representation. (B) The resulting $F_o - F_c$ electron density map obtained by omitting the magnesium ion from the final ADP bound structure is displayed contoured to 3σ showing strong positive electron density at the Mg2 site with no density for the Mg1 site. The ternary structure, 1RDQ,[7] colored olive was aligned by the entire protein to the ADP bound structure to illustrate the location of Asn171, Asp184, ATP, and the magnesium ions from the ternary structure.

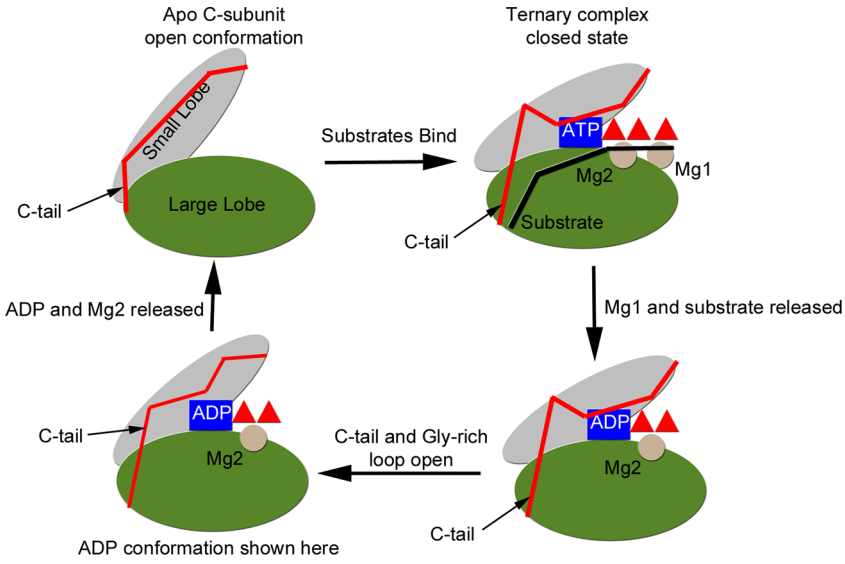

Figure 7. Schematic representation of possible steps and conformations involved in reaction turnover by PKA. This depiction highlights conformational changes that may occur including opening of the active site following substrate release. See Bastidas et al.[22] and Jacobsen et al.[23] for more detailed depictions of possible substrate binding and release steps.

bind the magnesium ions in positions that do not correspond to the Mg2 and Mg1 sites seen in PKA,[42,43] and there are structures with only one magnesium ion bound that binds only to ADP and no amino acid residues.[44,45] Therefore, these magnesium binding sites and mode of magnesium release may not be universal for all kinases but likely control many kinases.

In addition to validating the potential mode of magnesium release during reaction turnover, the ADP bound structure also provides a glimpse of possible motions and conformations involved in ADP release. The ADP bound structure adopts a mostly open conformation, but it is still more closed than the apo state (Figure 5A–C). The Gly-rich loop lowers compared with the apo state to help bind to ADP at the active site but not as much as in the ternary, closed state. Similarly, the C-tail moves into the active site to bind to ADP with residues Phe327 and Tyr330, as in the closed state, but the C-tail does not move into the active site to the same extent in the ADP bound structure as in the intermediate or closed states (Figure 5A–C).

ADP release likely proceeds with opening of the enzyme cleft via rising of the Gly-rich loop and C-terminal tail as shown in the ADP bound structure (Figure 5A–C). Also, one of the molecules in the asymmetric unit, chain A, does not show the C-tail binding at the active site because it is blocked by a symmetry related molecule (Figure 3B). ADP is still present at the active site in chain A but is not as stably bound as in chain B based on electron density and B-factor values. Therefore, a possible mode of ADP release involves removal of the C-terminal tail from the active site following general opening of the active site, which then destabilizes ADP binding allowing for release. Combining the information about the role of the magnesium ions in ADP release, a potential mode of reaction progression and ADP release by PKA becomes evident. Following phosphoryl transfer, Mg1 is released, which destabilizes ADP binding. Subsequently, the active site opens through rising of the Gly-rich loop and disengagement of the C-terminal tail, which is no longer coupled to the Gly-rich loop. This uncoupling of the C-tail from the Gly-rich loop would

dx.doi.org/10.1021/bi500684c | *Biochemistry* 2015, 54, 2–10

further facilitate ADP release (Figure 7). It is also possible that ADP release is not controlled by movement of the C-tail alone but by the coordinated motions of both the C-tail and Gly-rich loop together. Therefore, these structures begin to explain how the rate limiting step of ADP release may proceed and identify conformations and movements involved in this process. Also, each of the two molecules in the ASU exemplify possible conformations and trajectories involved in this release step. Our recent elucidation of a community map for PKA shows clearly how the C-tail and β strands one and two function as an integrated community in the closed conformation, whereas this community is uncoupled in the apo conformation (McClendon, C. et al., manuscript in preparation).

In summary, the ADP bound structure reported here further defines the conformational flexibility of the C-subunit and does not conform to any of the previously defined states, open, closed, or intermediate. Furthermore, the ADP bound structure provides evidence of how reaction progression may proceed in PKA and kinases in general. ADP binds at the active site with only one magnesium ion corresponding to Mg2, which is consistent with previous reports suggesting that Mg1 is released following phosphoryl transfer, and release of Mg1 may be an important step that precedes ADP release. Additionally, the conformation adopted with the ADP bound structure presents evidence of the conformational changes that may precede ADP release during reaction turnover including opening of the active site by movement of the Gly-rich loop and C-tail away from the active site.

■ ASSOCIATED CONTENT

Supporting Information

Validation of the Mg2 position in the ADP-bound structure (4NTT), performed with the CheckMyMetal web server, a metal binding site validation server, showing that the Mg2 in chain A has a good metal−ligand distance distribution in comparison with Cambridge Structural Database but the Mg2 in chain B is poorly coordinated in both geometry and metal−ligand distance distribution, suggesting the dynamics feature of the chain B. This material is available free of charge via the Internet at http://pubs.acs.org.

■ AUTHOR INFORMATION

Corresponding Author

*Susan S. Taylor. Mailing address: 9500 Gilman Dr., La Jolla, CA 92093-0654. Telephone: 858-534-3677. Fax: 858-534-8193. E-mail: staylor@ucsd.edu.

Funding

The project described was supported by grants from the National Institutes of Health (Grant GM19301 to S.S.T. and Grant F31GM099415 to A.C.B.). Additionally, Adam C. Bastidas acknowledges funding through the Ford Foundation Diversity Fellowship.

Notes

The authors declare no competing financial interest.

■ ABBREVIATIONS

PKA, protein kinase A; C-subunit, catalytic subunit of PKA; R-subunit, regulatory subunit of PKA; myr, myristylated; PKI, protein kinase inhibitor; bicine, *N*,*N*-bis(2-hydroxyethyl)-glycine; MPD, 2-methyl-2,4-pentanediol

■ REFERENCES

(1) Manning, G., Whyte, D. B., Martinez, R., Hunter, T., and Sudarsanam, S. (2002) The protein kinase complement of the human genome. *Science 298*, 1912−1934.

(2) Johnson, D. A., Akamine, P., Radzio-Andzelm, E., Madhusudan, M., and Taylor, S. S. (2001) Dynamics of cAMP-dependent protein kinase. *Chem. Rev. 101*, 2243−2270.

(3) Kim, C., Cheng, C. Y., Saldanha, S. A., and Taylor, S. S. (2007) PKA-I holoenzyme structure reveals a mechanism for cAMP-dependent activation. *Cell 130*, 1032−1043.

(4) Knighton, D. R., Zheng, J. H., Ten Eyck, L. F., Xuong, N. H., Taylor, S. S., and Sowadski, J. M. (1991) Structure of a peptide inhibitor bound to the catalytic subunit of cyclic adenosine monophosphate-dependent protein kinase. *Science 253*, 414−420.

(5) Akamine, P., Madhusudan, Wu, J., Xuong, N. H., Ten Eyck, L. F., and Taylor, S. S. (2003) Dynamic features of cAMP-dependent protein kinase revealed by apoenzyme crystal structure. *J. Mol. Biol. 327*, 159−171.

(6) Zheng, J., Knighton, D. R., Xuong, N. H., Taylor, S. S., Sowadski, J. M., and Ten Eyck, L. F. (1993) Crystal structures of the myristylated catalytic subunit of cAMP-dependent protein kinase reveal open and closed conformations. *Protein Sci. 2*, 1559−1573.

(7) Yang, J., Ten Eyck, L. F., Xuong, N. H., and Taylor, S. S. (2004) Crystal structure of a cAMP-dependent protein kinase mutant at 1.26A: New insights into the catalytic mechanism. *J. Mol. Biol. 336*, 473−487.

(8) Narayana, N., Cox, S., Nguyen-huu, X., Ten Eyck, L. F., and Taylor, S. S. (1997) A binary complex of the catalytic subunit of cAMP-dependent protein kinase and adenosine further defines conformational flexibility. *Structure 5*, 921−935.

(9) Masterson, L. R., Shi, L., Metcalfe, E., Gao, J., Taylor, S. S., and Veglia, G. (2011) Dynamically committed, uncommitted, and quenched states encoded in protein kinase A revealed by NMR spectroscopy. *Proc. Natl. Acad. Sci. U. S. A. 108*, 6969−6974.

(10) Adams, J. A. (2001) Kinetic and catalytic mechanisms of protein kinases. *Chem. Rev. 101*, 2271−2290.

(11) Adams, J. A., and Taylor, S. S. (1993) Divalent metal ions influence catalysis and active-site accessibility in the cAMP-dependent protein kinase. *Protein Sci. 2*, 2177−2186.

(12) Lew, J., Taylor, S. S., and Adams, J. A. (1997) Identification of a partially rate-determining step in the catalytic mechanism of cAMP-dependent protein kinase: A transient kinetic study using stopped-flow fluorescence spectroscopy. *Biochemistry 36*, 6717−6724.

(13) Shaffer, J., and Adams, J. A. (1999) An ATP-linked structural change in protein kinase A precedes phosphoryl transfer under physiological magnesium concentrations. *Biochemistry 38*, 5572−5581.

(14) Shaffer, J., and Adams, J. A. (1999) Detection of conformational changes along the kinetic pathway of protein kinase A using a catalytic trapping technique. *Biochemistry 38*, 12072−12079.

(15) Cook, P. F., Neville, M. E., Jr., Vrana, K. E., Hartl, F. T., and Roskoski, R., Jr. (1982) Adenosine cyclic 3′,5′-monophosphate dependent protein kinase: Kinetic mechanism for the bovine skeletal muscle catalytic subunit. *Biochemistry 21*, 5794−5799.

(16) Khavrutskii, I. V., Grant, B., Taylor, S. S., and McCammon, J. A. (2009) A transition path ensemble study reveals a linchpin role for Mg(2+) during rate-limiting ADP release from protein kinase A. *Biochemistry 48*, 11532−11545.

(17) Bossemeyer, D., Engh, R. A., Kinzel, V., Ponstingl, H., and Huber, R. (1993) Phosphotransferase and substrate binding mechanism of the cAMP-dependent protein kinase catalytic subunit from porcine heart as deduced from the 2.0 A structure of the complex with Mn2+ adenylyl imidodiphosphate and inhibitor peptide PKI(5−24). *EMBO J. 12*, 849−859.

(18) Zheng, J., Knighton, D. R., ten Eyck, L. F., Karlsson, R., Xuong, N., Taylor, S. S., and Sowadski, J. M. (1993) Crystal structure of the catalytic subunit of cAMP-dependent protein kinase complexed with MgATP and peptide inhibitor. *Biochemistry 32*, 2154−2161.

(19) Shaltiel, S., Cox, S., and Taylor, S. S. (1998) Conserved water molecules contribute to the extensive network of interactions at the

active site of protein kinase A. *Proc. Natl. Acad. Sci. U. S. A. 95*, 484−491.
(20) Kovalevsky, A. Y., Johnson, H., Hanson, B. L., Waltman, M. J., Fisher, S. Z., Taylor, S., and Langan, P. (2012) Low- and room-temperature X-ray structures of protein kinase A ternary complexes shed new light on its activity. *Acta Crystallogr. D: Biol. Crystallogr. 68*, 854−860.
(21) Bao, Z. Q., Jacobsen, D. M., and Young, M. A. (2011) Briefly bound to activate: Transient binding of a second catalytic magnesium activates the structure and dynamics of CDK2 kinase for catalysis. *Structure 19*, 675−690.
(22) Bastidas, A. C., Deal, M. S., Steichen, J. M., Guo, Y., Wu, J., and Taylor, S. S. (2013) Phosphoryl transfer by protein kinase a is captured in a crystal lattice. *J. Am. Chem. Soc. 135*, 4788−4798.
(23) Jacobsen, D. M., Bao, Z. Q., O'Brien, P., Brooks, C. L., 3rd, and Young, M. A. (2012) Price to be paid for two-metal catalysis: Magnesium ions that accelerate chemistry unavoidably limit product release from a protein kinase. *J. Am. Chem. Soc. 134*, 15357−15370.
(24) Duronio, R. J., Jackson-Machelski, E., Heuckeroth, R. O., Olins, P. O., Devine, C. S., Yonemoto, W., Slice, L. W., Taylor, S. S., and Gordon, J. I. (1990) Protein N-myristoylation in *Escherichia coli*: reconstitution of a eukaryotic protein modification in bacteria. *Proc. Natl. Acad. Sci. U. S. A. 87*, 1506−1510.
(25) Bastidas, A. C., Deal, M. S., Steichen, J. M., Keshwani, M. M., Guo, Y., and Taylor, S. S. (2012) Role of N-terminal myristylation in the structure and regulation of cAMP-dependent protein kinase. *J. Mol. Biol. 422*, 215−229.
(26) Battye, T. G., Kontogiannis, L., Johnson, O., Powell, H. R., and Leslie, A. G. (2011) iMOSFLM: A new graphical interface for diffraction-image processing with MOSFLM. *Acta Crystallogr. D: Biol. Crystallogr. 67*, 271−281.
(27) McCoy, A. J., Grosse-Kunstleve, R. W., Adams, P. D., Winn, M. D., Storoni, L. C., and Read, R. J. (2007) Phaser crystallographic software. *J. Appl. Crystallogr. 40*, 658−674.
(28) Collaborative Computational Project, Number 4 (1994) The CCP4 suite: programs for protein crystallography. *Acta Crystallogr. D Biol. Crystallogr. 50*, 760−763.
(29) Emsley, P., and Cowtan, K. (2004) Coot: model-building tools for molecular graphics. *Acta Crystallogr. D: Biol. Crystallogr. 60*, 2126−2132.
(30) Davis, I. W., Leaver-Fay, A., Chen, V. B., Block, J. N., Kapral, G. J., Wang, X., Murray, L. W., Arendall, W. B., 3rd, Snoeyink, J., Richardson, J. S., et al. (2007) MolProbity: All-atom contacts and structure validation for proteins and nucleic acids. *Nucleic Acids Res. 35*, W375−383.
(31) Nelson, N. C., and Taylor, S. S. (1981) Differential labeling and identification of the cysteine-containing tryptic peptides of catalytic subunit from porcine heart cAMP-dependent protein kinase. *J. Biol. Chem. 256*, 3743−3750.
(32) Batkin, M., Schvartz, I., and Shaltiel, S. (2000) Snapping of the carboxyl terminal tail of the catalytic subunit of PKA onto its core: Characterization of the sites by mutagenesis. *Biochemistry 39*, 5366−5373.
(33) Yang, J., Kennedy, E. J., Wu, J., Deal, M. S., Pennypacker, J., Ghosh, G., and Taylor, S. S. (2009) Contribution of non-catalytic core residues to activity and regulation in protein kinase A. *J. Biol. Chem. 284*, 6241−6248.
(34) Kennedy, E. J., Yang, J., Pillus, L., Taylor, S. S., and Ghosh, G. (2009) Identifying Critical Non-Catalytic Residues that Modulate Protein Kinase A Activity. *PLoS One 4* (3), No. e4746, DOI: 10.1371/journal.pone.0004746.
(35) Hyeon, C., Jennings, P. A., Adams, J. A., and Onuchic, J. N. (2009) Ligand-induced global transitions in the catalytic domain of protein kinase A. *Proc. Natl. Acad. Sci. U. S. A. 106*, 3023−3028.
(36) Kikani, C. K., Antonysamy, S. A., Bonanno, J. B., Romero, R., Zhang, F. F., Russell, M., Gheyi, T., Iizuka, M., Emtage, S., Sauder, J. M., et al. (2010) Structural bases of PAS domain-regulated kinase (PASK) activation in the absence of activation loop phosphorylation. *J. Biol. Chem. 285*, 41034−41043.
(37) Lawrence, H. R., Martin, M. P., Luo, Y., Pireddu, R., Yang, H., Gevariya, H., Ozcan, S., Zhu, J. Y., Kendig, R., Rodriguez, M., et al. (2012) Development of o-chlorophenyl substituted pyrimidines as exceptionally potent aurora kinase inhibitors. *J. Med. Chem. 55*, 7392−7416.
(38) Aoki, M., Yokota, T., Sugiura, I., Sasaki, C., Hasegawa, T., Okumura, C., Ishiguro, K., Kohno, T., Sugio, S., and Matsuzaki, T. (2004) Structural insight into nucleotide recognition in tau-protein kinase I/glycogen synthase kinase 3 beta. *Acta Crystallogr. D: Biol. Crystallogr. 60*, 439−446.
(39) Fischmann, T. O., Smith, C. K., Mayhood, T. W., Myers, J. E., Reichert, P., Mannarino, A., Carr, D., Zhu, H., Wong, J., Yang, R. S., et al. (2009) Crystal structures of MEK1 binary and ternary complexes with nucleotides and inhibitors. *Biochemistry 48*, 2661−2674.
(40) Hughes, S., Elustondo, F., Di Fonzo, A., Leroux, F. G., Wong, A. C., Snijders, A. P., Matthews, S. J., and Cherepanov, P. (2012) Crystal structure of human CDC7 kinase in complex with its activator DBF4. *Nat. Struct. Mol. Biol. 19*, 1101−1107.
(41) McNamara, L. K., Watterson, D. M., and Brunzelle, J. S. (2009) Structural insight into nucleotide recognition by human death-associated protein kinase. *Acta Crystallogr. D: Biol. Crystallogr. 65*, 241−248.
(42) Ko, T. P., Jeng, W. Y., Liu, C. I., Lai, M. D., Wu, C. L., Chang, W. J., Shr, H. L., Lu, T. J., and Wang, A. H. (2010) Structures of human MST3 kinase in complex with adenine, ADP and Mn2+. *Acta Crystallogr. D: Biol. Crystallogr. 66*, 145−154.
(43) Singh, P., Wang, B., Maeda, T., Palczewski, K., and Tesmer, J. J. (2008) Structures of rhodopsin kinase in different ligand states reveal key elements involved in G protein-coupled receptor kinase activation. *J. Biol. Chem. 283*, 14053−14062.
(44) Richards, M. W., O'Regan, L., Mas-Droux, C., Blot, J. M., Cheung, J., Hoelder, S., Fry, A. M., and Bayliss, R. (2009) An autoinhibitory tyrosine motif in the cell-cycle-regulated Nek7 kinase is released through binding of Nek9. *Mol. Cell 36*, 560−570.
(45) Westwood, I., Cheary, D. M., Baxter, J. E., Richards, M. W., van Montfort, R. L., Fry, A. M., and Bayliss, R. (2009) Insights into the conformational variability and regulation of human Nek2 kinase. *J. Mol. Biol. 386*, 476−485.